

Graphene: carbon in two dimensions

Carbon is one of the most intriguing elements in the Periodic Table. It forms many allotropes, some known from ancient times (diamond and graphite) and some discovered 10-20 years ago (fullerenes and nanotubes). Interestingly, the two-dimensional form (graphene) was only obtained very recently, immediately attracting a great deal of attention. Electrons in graphene, obeying a linear dispersion relation, behave like massless relativistic particles. This results in the observation of a number of very peculiar electronic properties – from an anomalous quantum Hall effect to the absence of localization – in this, the first two-dimensional material. It also provides a bridge between condensed matter physics and quantum electrodynamics, and opens new perspectives for carbon-based electronics.

Mikhail I. Katsnelson

Institute for Molecules and Materials, Radboud University Nijmegen, 6525 ED Nijmegen, The Netherlands

E-mail: katsnel@sci.kun.nl

Carbon plays a unique role in nature. The formation of carbon in stars as a result of the merging of three α -particles is a crucial process that leads to the existence of all the relatively heavy elements in the universe¹. The capability of carbon atoms to form complicated networks² is fundamental to organic chemistry and the basis for the existence of life, at least in its known forms. Even elemental carbon demonstrates unusually complicated behavior, forming a number of very different structures. As well as diamond and graphite, which have been known since ancient times, recently discovered fullerenes³⁻⁵ and nanotubes⁶ are currently a focus of attention for many physicists and chemists. Thus, only three-dimensional (diamond, graphite), one-dimensional (nanotubes),

and zero-dimensional (fullerenes) allotropes of carbon were known. The *two-dimensional* form was conspicuously missing, resisting any attempt at experimental observation – until recently.

A two-dimensional form of carbon

The elusive two-dimensional form of carbon is named graphene, and, ironically, it is probably the best-studied carbon allotrope theoretically. Graphene – planar, hexagonal arrangements of carbon atoms (Fig. 1) – is the starting point for all calculations on graphite, carbon nanotubes, and fullerenes. At the same time, numerous attempts to synthesize these two-dimensional atomic crystals have usually failed, ending up with nanometer-size crystallites⁷. These difficulties are not surprising in

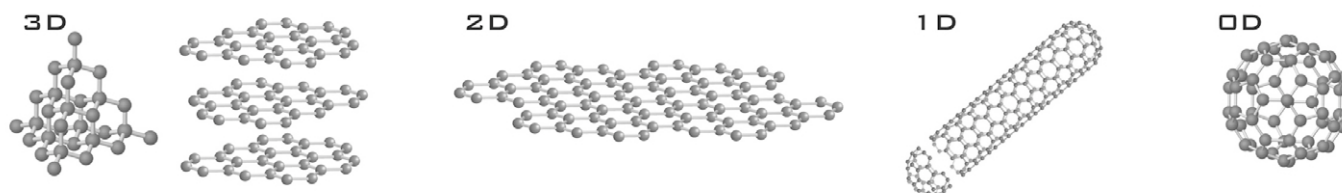


Fig. 1 Crystal structures of the different allotropes of carbon. (Left to right) Three-dimensional diamond and graphite (3D); two-dimensional graphene (2D); one-dimensional nanotubes (1D); and zero-dimensional buckyballs (0D). (Adapted and reprinted with permission from⁶⁶. © 2002 Prentice Hall.)

light of the common belief that truly two-dimensional crystals cannot exist⁸⁻¹² (in contrast to the numerous, known *quasi*-two-dimensional systems). Moreover, during synthesis, any graphene nucleation sites will have very large perimeter-to-surface ratios, thus promoting collapse into other carbon allotropes.

Discovery of graphene

In 2004, a group of physicists from Manchester University, UK, led by Andre Geim and Kostya Novoselov, used a very different and, at first glance, even naive approach to obtain graphene and lead a revolution in the field. They started with three-dimensional graphite and extracted a single sheet (a monolayer of atoms) using a technique called micromechanical cleavage^{13,14} (Fig. 2). Graphite is a layered material and can be viewed as a number of two-dimensional graphene crystals weakly coupled together – exactly the property used by the Manchester team. By using this top-down approach and starting with large, three-dimensional crystals, the researchers avoided all the issues with the stability of small crystallites. Furthermore, the same technique has been used by the group to obtain two-dimensional crystals of other materials¹³, including boron nitride, some dichalcogenides, and the high-temperature superconductor Bi-Sr-Ca-Cu-O. This astonishing finding sends an important message: two-dimensional crystals do exist and they are stable under ambient conditions.

Amazingly, this humble approach allows easy production of large (up to 100 μm in size), high-quality graphene crystallites,

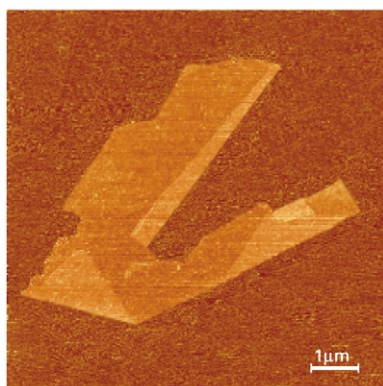


Fig. 2 Atomic force microscopy image of a graphene crystal on top of an oxidized Si substrate. Folding of the flake can be seen. The measured thickness of graphene corresponds to the interlayer distance in graphite. Scale bar = 1 μm . (Reprinted with permission from¹³. © 2005 National Academy of Sciences.)

and immediately triggered enormous experimental activity^{15,16}. Moreover, the quality of the samples produced are so good that ballistic transport¹⁴ and a quantum Hall effect (QHE) can be observed easily^{15,16}. The former makes this new material a promising candidate for future electronic applications, such as ballistic field-effect transistors (FETs). However, while this approach suits all research needs, other techniques that provide a high yield of graphene are required for industrial production. Among the promising candidate methods, one should mention exfoliation of intercalated graphitic compounds¹⁷⁻²¹ and Si sublimation from SiC substrates, demonstrated recently by Walt de Heer's group at Georgia Institute of Technology²².

Stability in two dimensions

The fact that two-dimensional atomic crystals do exist, and moreover, are stable under ambient conditions¹³ is amazing by itself. According to the Mermin-Wagner theorem¹², there should be no long-range order in two dimensions. Thus, dislocations should appear in two-dimensional crystals at any finite temperature.

A standard description²³ of atomic motion in solids assumes that amplitudes of atomic vibration \bar{u} near their equilibrium position are much smaller than interatomic distances d , otherwise the crystal would melt according to an empirical Lindemann criterion (at the melting point, $\bar{u} \approx 0.1d$). As a result of this small amplitude, the thermodynamics of solids can be successfully described using a picture of an ideal gas of phonons, i.e. quanta of atomic displacement waves (harmonic approximation). In three-dimensional systems, this view is self-consistent in a sense that fluctuations of atomic positions calculated in the harmonic approximation do indeed turn out to be small, at least at low enough temperatures. In contrast, in a two-dimensional crystal, the number of long-wavelength phonons diverges at low temperatures and, thus, the amplitudes of interatomic displacements calculated in the harmonic approximation diverge⁸⁻¹⁰.

According to similar arguments, a flexible membrane embedded in three-dimensional space should be crumpled because of dangerous long-wavelength bending fluctuations²⁴. However, in the past 20 years, theoreticians have demonstrated that these dangerous fluctuations can be suppressed by anharmonic (nonlinear) coupling between bending and stretching modes²⁴⁻²⁶. As a result, single-crystalline membranes can exist but should be 'rippled'. This gives rise to 'roughness fluctuations' with a typical height that scales with sample size L as L^ζ , with $\zeta \approx 0.6$. Indeed, ripples are observed in graphene, and

play an important role in its electronic properties²⁷. However, these investigations have just started (there are a few recent papers on Raman spectroscopy of graphene^{28,29}), and 'phononic' aspects of two-dimensionality in graphene are still very poorly understood.

Another important issue is the role of defects in the thermodynamic stability of two-dimensional crystals. Finite concentrations of dislocations and disclinations would destroy long-range translational and orientational order, respectively. A detailed analysis²⁴ shows that dislocations in *flexible* membranes have finite energy (of the order of the cohesion energy E_{coh}) caused by screening of the bending deformations, whereas the energy of disclinations is logarithmically divergent with the size of crystallite. This means that, rigorously speaking, the translational long-range order (but not orientational order) is broken at any finite temperature T . However, the density of dislocations in the equilibrium is exponentially small for large enough E_{coh} (in comparison with the thermal energy $k_B T$) so, in practice, this restriction is not very serious for strongly bonded two-dimensional crystals like graphene.

Electronic structure of graphene

The electronic structure of graphene follows from a simple nearest-neighbor, tight-binding approximation³⁰. Graphene has two atoms per unit cell, which results in two 'conical' points per Brillouin zone where band crossing occurs, K and K' . Near these crossing points, the electron energy is linearly dependent on the wave vector. Actually, this behavior follows from symmetry considerations³¹, and thus is robust with respect to long-range hopping processes (Fig. 3).

What makes graphene so attractive for research is that the spectrum closely resembles the Dirac spectrum for massless fermions^{32,33}. The Dirac equation describes relativistic quantum

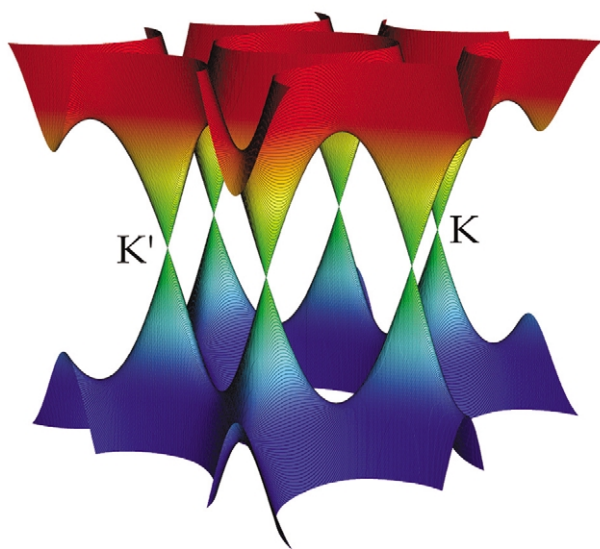


Fig. 3 Band structure of graphene. The conduction band touches the valence band at the K and K' points.

particles with spin $\frac{1}{2}$, such as electrons. The essential feature of the Dirac spectrum, following from the basic principles of quantum mechanics and relativity theory, is the existence of antiparticles. More specifically, states at positive and negative energies (electrons and positrons) are intimately linked (conjugated), being described by different components of the same spinor wave function. This fundamental property of the Dirac equation is often referred to as the charge-conjugation symmetry. For Dirac particles with mass m , there is a gap between the minimal electron energy, $E_0 = mc^2$, and the maximal positron energy, $-E_0$ (c is the speed of light). When the electron energy $E \gg E_0$, the energy is linearly dependent on the wavevector k , $E = \hbar k v_F$. For massless Dirac fermions, the gap is zero and this linear dispersion law holds at any energy. In this case, there is an intimate relationship between the spin and motion of the particle: spin can only be directed along the propagation direction (say, for particles) or only opposite to it (for antiparticles). In contrast, massive spin- $\frac{1}{2}$ particles can have two values of spin projected onto any axis. In a sense, we have a unique situation here: charged massless particles. Although this is a popular textbook example, no such particles have been observed before.

The fact that charge carriers in graphene are described by a Dirac-like spectrum, rather than the usual Schrödinger equation for nonrelativistic quantum particles, can be seen as a consequence of graphene's crystal structure. This consists of two equivalent carbon sublattices A and B (see Fig. 4). Quantum-mechanical hopping between the sublattices leads to the formation of two energy bands, and their intersection near the edges of the Brillouin zone yields the conical energy spectrum. As a result, quasiparticles in graphene exhibit a linear dispersion relation $E = \hbar k v_F$, as if they were massless relativistic particles (for example, photons) but the role of the speed of light is played here by the Fermi velocity $v_F \approx c/300$. Because of the linear spectrum, one can expect that quasiparticles in graphene behave differently from those in conventional metals and semiconductors, where the energy spectrum can be approximated by a parabolic (free-electron-like) dispersion relation.

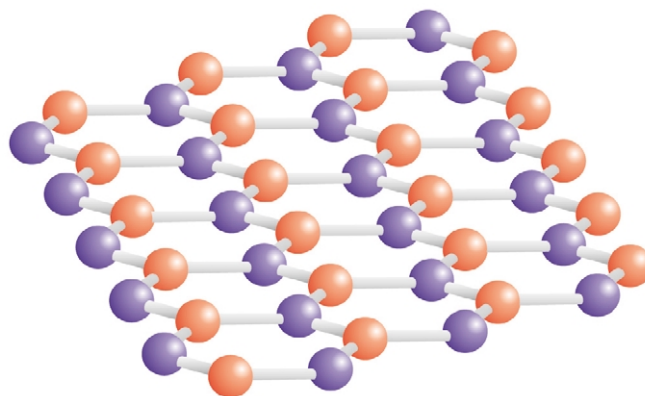


Fig. 4 Crystallographic structure of graphene. Atoms from different sublattices (A and B) are marked by different colors.

Chiral Dirac electrons

Although graphene's linear spectrum is important, it is not the spectrum's only essential feature. Above zero energy, the current-carrying states in graphene are, as usual, electron-like and negatively charged. At negative energies, if the valence band is not full, unoccupied electronic states behave as positively charged quasiparticles (holes), which are often viewed as a condensed matter equivalent of positrons. Note, however, that electrons and holes in condensed matter physics are normally described by separate Schrödinger equations, which are not in any way connected (as a consequence of the so-called Seitz sum rule³⁴, the equations should also involve different effective masses). In contrast, electron and hole states in graphene should be interconnected, exhibiting properties analogous to the charge-conjugation symmetry in quantum electrodynamics (QED)³¹⁻³³.

For the case of graphene, the latter symmetry is a consequence of the crystal symmetry, because graphene's quasiparticles have to be described by two-component wave functions, which are needed to define the relative contributions of the A and B sublattices in the quasiparticles' make-up. The two-component description for graphene is very similar to the spinor wave functions in QED, but the 'spin' index for graphene indicates the sublattice rather than the real spin of the electrons and is usually referred to as pseudospin σ . This allows one to introduce chirality³³ – formally a projection of pseudospin on the direction of motion – which is positive and negative for electrons and holes, respectively.

The description of the electron spectrum of graphene in terms of Dirac massless fermions is a kind of continuum-medium description applicable for electron wavelengths much larger than interatomic distances. However, even at these length scales, there is still some retention of the structure of the elementary cell, that is, the existence of two sublattices. In terms of continuum field theory, this can be described only as an *internal* degree of freedom of the charge carriers, which is just the chirality.

This description is based on an oversimplified nearest-neighbor tight-binding model. However, it has been proven experimentally that charge carriers in graphene do have this Dirac-like gapless energy spectrum^{15,16}. This was demonstrated in transport experiments (Fig. 5) via investigation of the Schubnikov-de Haas effect, i.e. resistivity oscillations at high magnetic fields and low temperatures.

Anomalous quantum Hall effect

Magneto-oscillation effects, such as the de Haas-van Alphen (oscillations of magnetization) or Schubnikov-de Haas (magneto-oscillations in resistance) effects, are among the most straightforward and reliable tools to investigate electron energy spectra in metals and semiconductors³⁵. In two-dimensional systems with a constant magnetic field \mathbf{B} perpendicular to the system plane, the energy spectrum is discrete (Landau quantization). In the case of massless

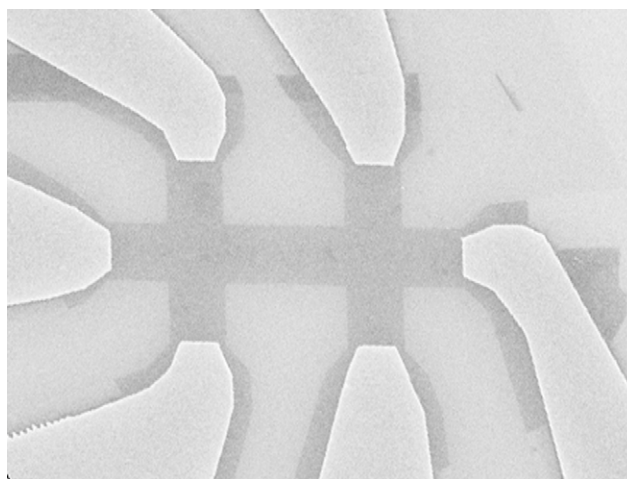


Fig. 5 Scanning electron micrograph of a graphene device. The graphene crystal is contacted by Au electrodes and patterned into Hall bar geometry by e-beam lithography with subsequent reactive plasma etching. The width of the channel is 1 μm . (Courtesy of K. Novoselov and A. Geim.)

Dirac fermions, the energy spectrum takes the form (see³⁶, for example):

$$E_{\nu\sigma} = \pm \sqrt{2|e|B\hbar v_F^2(\nu + 1/2 \pm 1/2)} \quad (1)$$

where v_F is the electron velocity, $\nu = 0, 1, 2, \dots$ is the quantum number, and the term with $\pm 1/2$ is connected with the chirality (Fig. 6). For comparison, in the usual case of a parabolic dispersion relation, the Landau level sequence is $E = \hbar\omega_c(\nu + 1/2)$ where ω_c is the frequency of electron rotation in the magnetic field (cyclotron frequency)³⁵.

By changing the value of the magnetic field at a given electron concentration (or, vice versa, electron concentration for a given magnetic field), one can tune the Fermi energy E_F to coincide with one of the Landau levels. This drastically changes all properties of metals (or semiconductors) and, thus, different physical quantities will oscillate with the value of the inverse magnetic field. By measuring the period

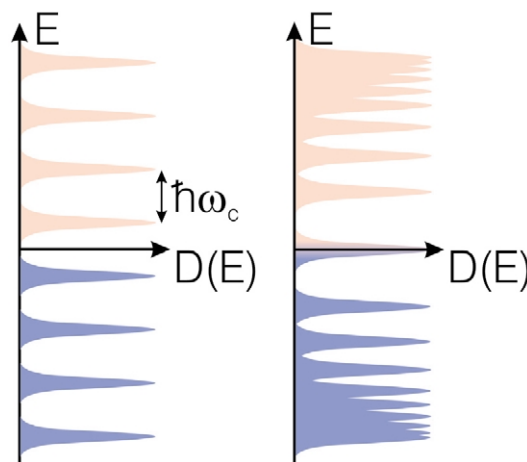


Fig. 6 (Left) Landau levels for Schrödinger electrons with two parabolic bands touching each other at zero energy. (Right) Landau levels for Dirac electrons.

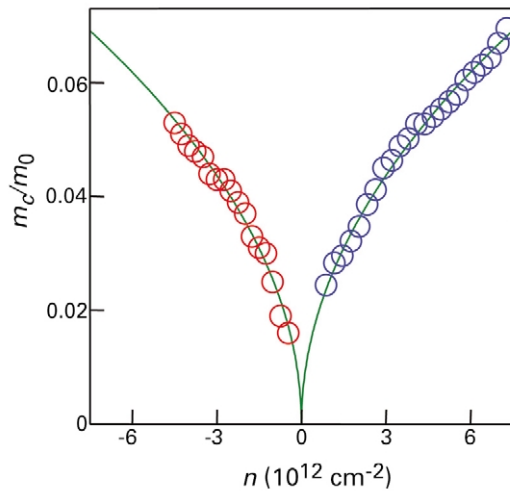


Fig. 7 Electron and hole cyclotron mass as a function of carrier concentration in graphene. The square-root dependence suggests a linear dispersion relation. (Reprinted with permission from¹⁵. © 2005 Nature Publishing Group.)

of these oscillations $\Delta(1/B)$, we obtain information about the area A inside the Fermi surface (for two-dimensional systems, this area is just proportional to the charge-carrier concentration n). The amplitude of the oscillations allows us to measure the effective cyclotron mass which is proportional to $\partial A/\partial E_F$ ^{34,35}. For the case of massless Dirac fermions (linear dependence of the electron energy on its momentum), this quantity should be proportional to \sqrt{n} , which was exactly the behavior reported simultaneously by the Manchester researchers¹⁵ and Philip Kim and Horst Stormer's group at Columbia University¹⁶ (Fig. 7).

An important peculiarity of the Landau levels for massless Dirac fermions is the existence of zero-energy states (with $\nu = 0$ and a minus sign in eq. 1). This situation differs markedly from conventional semiconductors with parabolic bands where the first Landau level is shifted by $\frac{1}{2}\hbar\omega_c$. As shown by the Manchester and Columbia groups^{15,16}, the existence of the zero-energy Landau level leads to an anomalous QHE with *half-integer* quantization of the Hall conductivity (Fig. 8, top), instead of an *integer* one (for a review of the QHE, see³⁷, for example). Usually, all Landau levels have the same degeneracy (number of electron states with a given energy), which is proportional to the magnetic flux through the system. As a result, the plateaus in the Hall conductivity corresponding to the filling of first ν levels are integers (in units of the conductance quantum e^2/h). For the case of massless Dirac electrons, the zero-energy Landau level has half the degeneracy of any other level (corresponding to the minus sign in eq. 1), whereas each p^{th} level with $p \geq 1$ is obtained twice, with $\nu = p$ and a minus sign, and with $\nu = p - 1$ and a plus sign. This anomalous QHE is the most direct evidence for Dirac fermions in graphene^{15,16}.

Index theorem

The deepest view on the origin of the zero-energy Landau level, and thus the anomalous QHE is provided by an Atiyah-Singer index, theorem that plays an important role in modern quantum field

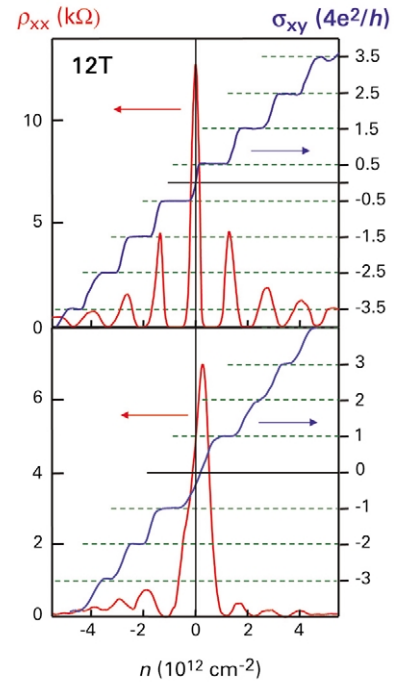


Fig. 8 Resistivity (red) and Hall conductivity (blue) as a function of carrier concentration in graphene (top) and bilayer graphene (bottom). (Reprinted with permission from¹⁵ (top) and from⁴⁷ (bottom). © 2005 and 2006 Nature Publishing Group.)

theory and theory of superstrings³⁸. The Dirac equation has charge-conjugation symmetry between electrons and holes. This means that, for any electron state with a positive energy E , a corresponding conjugated hole state with energy $-E$ should exist. However, states with zero energy can be, in general, anomalous. For curved space (e.g. for a deformed graphene sheet with some defects in crystal structure) and/or in the presence of so-called 'gauge fields' (electromagnetic fields provide the simplest example of these fields), sometimes the existence of states with zero energy is guaranteed for topological reasons, these states being chiral. (In the case of graphene, this means that, depending on the sign of the magnetic field, only sublattice A or sublattice B states contribute to the zero-energy Landau level.) In particular, this means that the number of these states expressed in terms of total magnetic flux is a topological invariant and remains the same even if the magnetic field is inhomogeneous¹⁵. This is an important conclusion since the ripples on graphene create effective inhomogeneous magnetic fields with magnitudes up to 1 T, leading to suppression of the weak localization²⁷. However, because of these topological arguments, inhomogeneous magnetic fields cannot destroy the anomalous QHE in graphene. For further insight into the applications of the index theorem to two-dimensional systems, and to graphene in particular, see^{39,40}.

Quasiclassical considerations

An alternative view of the origin of the anomalous QHE in graphene is based on the concept of a 'Berry phase'⁴¹. Since the electron wave

function is a two-component spinor, it has to change sign when the electron moves along a closed contour. Thus, the wave function gains an additional phase $\phi = \pi$. In quasiclassical terms (see^{34,42}, for example), stationary states are nothing but electron standing waves and they can exist if the electron orbit is, at least, half the wavelength. As a result of the additional phase shift by the Berry phase, this condition is already satisfied for the zeroth length of the orbit, that is, for zero energy! Other aspects of the QHE in graphene are considered elsewhere⁴³⁻⁴⁶.

Anomalous QHE in bilayer graphene

In relativistic quantum mechanics, chirality is intimately connected with relativistic considerations that dictate, at the same time, the linear energy spectrum for massless particles. The discovery of graphene also opens a completely new opportunity to investigate *chiral* particles with a *parabolic* (*nonrelativistic*) energy spectrum! This is the case for *bilayer* graphene⁴⁷.

For two carbon layers, the nearest-neighbor tight-binding approximation predicts a gapless state with *parabolic* bands touching at the *K* and *K'* points, instead of conical bands^{47,48}. More accurate consideration⁴⁹ gives a very small band overlap (about 1.6 meV) but, at larger energies, bilayer graphene can be treated as a gapless semiconductor. At the same time, the electron states are still characterized by chirality and by the Berry phase (equal, in this case, to 2π instead of π). Exact solution of the quantum mechanical equation for this kind of spectrum in the presence of a homogeneous magnetic field gives the result^{47,48} $E_v \propto \sqrt{v(v-1)}$ and, thus, the number of states with zero energy ($v = 0$ and $v = 1$) is twice that of monolayer graphene. As a result, the QHE for bilayer graphene differs from both single-layer graphene and conventional semiconductors, as found experimentally⁴⁷ (Fig. 8, bottom).

Tunneling of chiral particles

The chiral nature of electron states in bilayer, as well as single-layer, graphene is of crucial importance for electron tunneling through potential barriers, and thus the physics of electronic devices such as 'carbon transistors'⁵⁰.

Quantum tunneling

Quantum tunneling is a consequence of very general laws of quantum mechanics, such as the Heisenberg uncertainty relations. A classical particle cannot propagate through a region where its potential energy is higher than its total energy (Fig. 9). However, because of the uncertainty principle, it is impossible to know the exact values of a quantum particle's coordinates and velocity, and thus its kinetic and potential energy, at the same time instant. Therefore, penetration through the 'classically forbidden' region turns out to be possible. This phenomenon is widely used in modern electronics, beginning with the pioneering work of Esaki⁵¹.

Klein paradox

When a potential barrier is smaller than the gap separating electron and hole bands in semiconductors, the penetration probability decays exponentially with the barrier height and width. Otherwise, resonant tunneling is possible when the energy of the propagating electron coincides with one of the hole energy levels inside the barrier. Surprisingly, in the case of graphene, the transmission probability for normally incident electrons is always equal to unity, irrespective of the height and width of the barrier^{50,52,53}.

In QED, this behavior is related to the Klein paradox^{50,54-56}. This phenomenon usually refers to a counterintuitive relativistic process in which an incoming electron starts penetrating through a potential barrier, if the barrier height exceeds twice the electron's rest energy mc^2 . In this case, the transmission probability T depends only weakly on barrier height, approaching perfect transparency for very high barriers, in stark contrast to conventional, nonrelativistic tunneling. This relativistic effect can be attributed to the fact that a sufficiently strong potential, being repulsive for electrons, is attractive to positrons, and results in positron states inside the barrier. These align in energy with the electron continuum outside the barrier. Matching between electron and positron wave functions across the barrier leads to the high-probability tunneling described by the Klein paradox. In other words, it reflects an essential difference between nonrelativistic and relativistic quantum mechanics. In the former case, we can measure accurately either the position of the electron or its velocity, but not both simultaneously. In relativistic quantum mechanics, we cannot measure even electron position with arbitrary accuracy since, if we try to do this, we create electron-positron pairs from the vacuum and we cannot distinguish our original electron from these newly created electrons. Graphene opens a way to investigate this counterintuitive behavior in a relatively simple benchtop experiment, whereas previously the Klein paradox was only connected with some very exotic phenomena, such

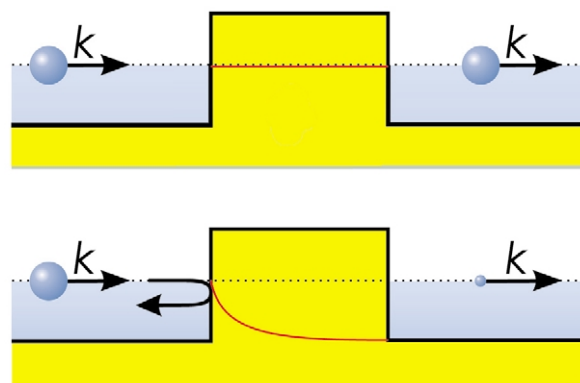


Fig. 9 Tunneling in graphene (top) and conventional semiconductors (bottom). The amplitude of the electron wave function (red) remains constant in graphene while it decays exponentially in conventional tunneling. The size of the sphere indicates the amplitude of the incident and transmitted wave functions. (Reprinted with permission from⁵⁰. © 2006 Nature Publishing Group.)

as collisions of ultraheavy nuclei or black hole evaporations (for more references and explanations, see^{50,56}).

Tunneling in bilayer graphene

From the point of view of applications, the Klein paradox is rather bad news since it means that a 'carbon transistor' using single-layer graphene cannot be closed by any external gate voltage. In contrast, it has been shown that chiral tunneling in the case of a *bilayer* leads to even stronger suppression of the normally incident electron penetration (Fig. 10) than in conventional semiconductors⁵⁰. By creating a potential barrier (with an external gate), one can manipulate the transmission probability for ballistic electrons in bilayer graphene. At the same time, there is always some 'magic angle' where the penetration probability equals unity (Fig. 10), which also should be taken into account in the design of future carbon-based electronic devices.

Absence of localization

The tunneling anomalies in single- and bilayer graphene systems are expected to play an important role in their transport properties, especially in the regime of low carrier concentrations where disorder induces significant potential barriers and the systems are likely to split into a random distribution of *p-n* junctions. In conventional two-dimensional systems, sufficiently strong disorder results in electronic states that are separated by barriers with exponentially small transparency^{57,58}. This is known to lead to Anderson localization. In contrast, in both graphene materials, all potential barriers are rather transparent, at least for some angles. This means that charge carriers

cannot be confined by potential barriers that are smooth on the atomic scale. Therefore, different electron and hole 'puddles' induced by disorder are not isolated but effectively percolate, thereby suppressing localization. This is important in understanding the minimal conductivity $\approx e^2/h$ observed experimentally in both single-¹⁵ and bilayer⁴⁷ graphene. Further discussion of this minimal conductivity phenomenon in terms of quantum relativistic effects can be found elsewhere⁵⁹⁻⁶¹.

Graphene devices

The unusual electronic properties of this new material make it a promising candidate for future electronic applications. Mobilities that are easily achieved at the current state of 'graphene technology' are $\sim 20\,000\text{ cm}^2/\text{V}\cdot\text{s}$, which is already an order of magnitude higher than that of modern Si transistors, and they continue to grow as the quality of samples improves. This ensures ballistic transport on submicron distances – the holy grail for any electronic engineer. Probably the best candidates for graphene-based FETs will be devices based on quantum dots and those using *p-n* junctions in bilayer graphene^{50,62}.

Another promising direction for investigation is spin-valve devices. Because of negligible spin-orbit coupling, spin polarization in graphene survives over submicron distances, which has recently allowed observation of spin-injection and a spin-valve effect in this material⁶³. It has also been shown by Morpurgo and coworkers at Delft University⁶⁴ that superconductivity can be induced in graphene through the proximity effect (Fig. 11). Moreover, the magnitude of the supercurrent can be controlled by an external gate voltage, which can be used to create a superconducting FET.

While these applications mentioned are a focus for further investigation, there are some areas where graphene can be used straightaway. Gas sensors is one. The Manchester group⁶⁵ has shown that graphene can absorb gas molecules from the surrounding atmosphere, resulting in doping of the graphene layer with electrons or holes depending on the nature of the absorbed gas. By monitoring

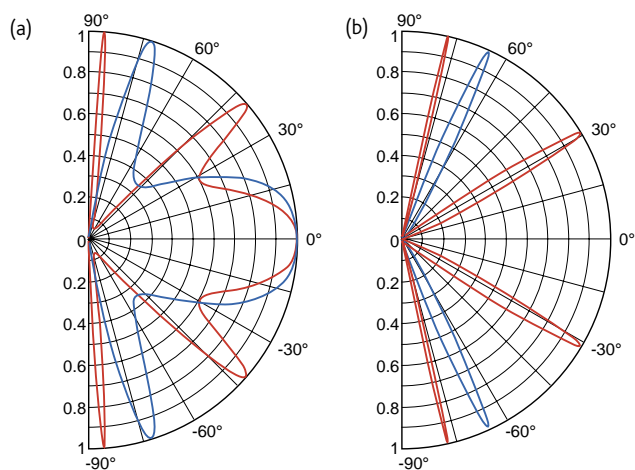


Fig. 10 Transmission probability T through a 100 nm wide barrier as a function of the incident angle for (a) single- and (b) bilayer graphene. The electron concentration n outside the barrier is chosen as $0.5 \times 10^{12}\text{ cm}^{-2}$ for all cases. Inside the barrier, hole concentrations p are 1×10^{12} and $3 \times 10^{12}\text{ cm}^{-2}$ for the red and blue curves, respectively (concentrations that are typical of most experiments with graphene). This corresponds to a Fermi energy E for the incident electrons of $\approx 80\text{ meV}$ and 17 meV for single- and bilayer graphene, respectively, and $\lambda \approx 50\text{ nm}$. The barrier heights are (a) 200 meV and (b) 50 meV (red curves), and (a) 285 meV and (b) 100 meV (blue curves).

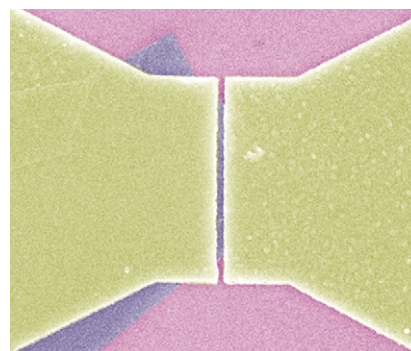


Fig. 11 Scanning electron micrograph of a graphene crystal contacted by superconducting electrodes. Supercurrents arising from the proximity effect have been observed recently by researchers in Delft, the Netherlands⁶⁴. The gap between the electrodes is 70 nm.

changes in resistivity, one can sense minute concentrations of certain gases present in the environment.

Conclusions

It is impossible to review all aspects of graphene physics and chemistry here. We hope, however, that the above examples demonstrate graphene's great interest for both fundamental research (where it forms a new, unexpected bridge between condensed matter and quantum field theory) and possible applications. Graphene is the first example of a truly two-dimensional crystal. This opens many interesting questions concerning the thermodynamics, lattice dynamics, and structural properties of such systems. Being a gapless semiconductor with a linear energy spectrum, single-layer graphene

realizes a two-dimensional, massless Dirac fermion system that is of crucial importance for understanding unusual electronic properties, such as an anomalous QHE, absence of the Anderson localization, etc. Bilayer graphene has a very unusual gapless, parabolic spectrum, giving a system with an electron wave equation that is different from both Dirac and Schrödinger systems. These peculiarities are important for developing new electronic devices such as carbon transistors. 

Acknowledgments

I am thankful to Kostya Novoselov and Andre Geim for many helpful discussions. This work was supported by the Stichting voor Fundamenteel Onderzoek der Materie (FOM), the Netherlands.

REFERENCES

1. Fowler, W. A., *Rev. Mod. Phys.* (1984) **56**, 149
2. Pauling, L., *The Nature of the Chemical Bond*, Cornell University Press, Ithaca, NY, (1960)
3. Curl, R. F., *Rev. Mod. Phys.* (1997) **69**, 691
4. Kroto, H., *Rev. Mod. Phys.* (1997) **69**, 703
5. Smalley, R. E., *Rev. Mod. Phys.* (1997) **69**, 723
6. Iijima, S., *Nature* (1991) **354**, 56
7. Oshima, C., and Nagashima, A., *J. Phys.: Condens. Matter* (1997) **9**, 1
8. Peierls, R. E., *Helv. Phys. Acta* (1934) **7**, 81
9. Peierls, R. E., *Ann. Inst. H. Poincaré* (1935) **5**, 177
10. Landau, L. D., *Phys. Z. Sowjet Union* (1937) **11**, 26
11. Landau, L. D., and Lifshitz, E. M., *Statistical Physics, Part I*, Pergamon, Oxford, UK, (1980)
12. Mermin, N. D., *Phys. Rev.* (1968) **176**, 250
13. Novoselov, K. S., et al., *Proc. Natl. Acad. Sci. USA* (2005) **102**, 10451
14. Novoselov, K. S., et al., *Science* (2004) **306**, 666
15. Novoselov, K. S., et al., *Nature* (2005) **438**, 197
16. Zhang, Y., et al., *Nature* (2005) **438**, 201
17. Dresselhaus, M. S., and Dresselhaus, G., *Adv. Phys.* (2002) **51**, 1
18. Shioyama, H., *J. Mater. Sci. Lett.* (2001) **20**, 499
19. Viculis, L. M., et al., *Science* (2003) **299**, 1361
20. Horiuchi, S., et al., *Appl. Phys. Lett.* (2004) **84**, 2403
21. Stankovich, S., et al., *J. Mater. Chem.* (2006) **16**, 155
22. Berger, C., et al., *J. Phys. Chem. B* (2004) **108**, 19912
23. Born, M., and Huang, K., *Dynamical Theory of Crystal Lattices*, Oxford University Press, Oxford, UK (1998)
24. Nelson, D. R., et al., (eds.), *Statistical Mechanics of Membranes and Surfaces*, World Scientific, Singapore, (2004)
25. Nelson, D. R., and Peliti, L., *J. Physique* (1987) **48**, 1085
26. Le Doussal, P., and Radzihovsky, L., *Phys. Rev. Lett.* (1992) **69**, 1209
27. Morozov, S. V., et al., *Phys. Rev. Lett.* (2006) **97**, 016801
28. Ferrari, A. C., et al., *Phys. Rev. Lett.* (2006) **97**, 187401
29. Graf, D., et al., (2006), arxiv.org/pdf/cond-mat/0607562
30. Wallace, P. R., *Phys. Rev.* (1947) **71**, 622
31. Slonczewski, J. C., and Weiss, P. R., *Phys. Rev.* (1958) **109**, 272
32. Semenoff, G. W., *Phys. Rev. Lett.* (1984) **53**, 2449
33. Haldane, F. D. M., *Phys. Rev. Lett.* (1988) **61**, 2015
34. Vonsovsky, S. V., and Katsnelson, M. I., *Quantum Solid State Physics*, Springer, NY, (1989)
35. Ashcroft, N. W., and Mermin, N. D., *Solid State Physics*, Holt, Rinehart and Winston, NY, (1976)
36. Gusynin, V. P., and Sharapov, S. G., *Phys. Rev. B* (2005) **71**, 125124
37. Prange, R. E., and Girvin, S. M., (eds.), *The Quantum Hall Effect*, Springer, NY, (1987)
38. Kaku, M., *Introduction to Superstrings*, Springer, NY, (1988)
39. Tenjinbayashi, Y., et al., *Ann. Phys.* (2006) doi:10.1016/j.aop.2006.02.013
40. Pachs, J. K., and Stone, M., (2006), arxiv.org/pdf/cond-mat/0607394
41. Shapere, A., and Wilczek, F., (eds.), *Geometrical Phases in Physics*, World Scientific, Singapore, (1989)
42. Mikić, G. P., and Sharlai, Yu. V., *Phys. Rev. Lett.* (1999) **82**, 2147
43. Abanin, D. A., et al., *Phys. Rev. Lett.* (2006) **96**, 176803
44. Gusynin, V. P., and Sharapov, S. G., *Phys. Rev. Lett.* (2005) **95**, 146801
45. Peres, N. M. R., et al., *Phys. Rev. B* (2006) **73**, 125411
46. Castro Neto, A. H., et al., *Phys. Rev. B* (2006) **73**, 205408
47. Novoselov, K. S., et al., *Nat. Phys.* (2006) **2**, 177
48. McCann, E., and Fal'ko, V. I., *Phys. Rev. Lett.* (2006) **96**, 086805
49. Partoens, B., and Peeters, F. M., *Phys. Rev. B* (2006) **74**, 075404
50. Katsnelson, M. I., et al., *Nat. Phys.* (2006) **2**, 620
51. Esaki, L., *Phys. Rev.* (1958) **109**, 603
52. Milton Pereira, Jr., J., et al., *Phys. Rev. B* (2006) **74**, 045424
53. Cheianov, V. V., and Fal'ko, V. I., *Phys. Rev. B* (2006) **74**, 041403(R)
54. Klein, O., *Z. Phys.* (1929) **53**, 157
55. Dombey, N., and Calogeracos, A., *Phys. Rep.* (1999) **315**, 41
56. Calogeracos, A., *Nat. Phys.* (2006) **2**, 579
57. Ziman, J. M., *Models of Disorder*, Cambridge University Press, Cambridge, UK, (1979)
58. Lifshitz, I. M., et al., *Introduction to the Theory of Disordered Systems*, Wiley, NY, (1988)
59. Katsnelson, M. I., *Eur. Phys. J. B* (2006) **51**, 157
60. Katsnelson, M. I., *Eur. Phys. J. B* (2006) **52**, 151
61. Tworzydło, J., et al., *Phys. Rev. Lett.* (2006) **96**, 246802
62. Nilsson, J., et al., (2006), arxiv.org/pdf/cond-mat/0607343
63. Hill, E. W., et al., *IEEE Trans. Magn.* (2006) **42**, 2694
64. Heersche, H. B., et al., Presented at *Nanophysics: from Fundamentals to Applications*, Hanoi, Vietnam, August, 2006
65. Schedin, F., et al., (2006), arxiv.org/pdf/cond-mat/0610809
66. Hill, J. W., and Petrucci, R. H., *General Chemistry*, 3rd edition, Prentice Hall, NJ, (2002)